Journal of Gono Bishwabidyalay
ISSN: 2521-828X(Print)
2706-9303 (Online)
2706-9311(CD-ROM)
Journal Homepage: https://gonouniversity.edu.bd/research/journal-of-gb/

Original Research

Synthesis and Characterization of Reduced Graphene Oxide Reinforced Hydroxyapatite Composite for Biomedical Applications

Md. Tushar Ahmed[1*] and Md. Mostafa Kamal[1]

[1] Department of Physics, Gono Bishwabidyalay, Savar, Dhaka 1344.

*** Corresponding Author:** Md. Tushar Ahmed; Email: tusharahmed44@outlook.com; Mobile: +8801768660850.

Received: 26/06/ 2026; **Accepted**: 07/11/2026; **Online Available**: 12/11/2026.

Abstract

In this study, reduced graphene oxide – hydroxyapatite (RGO–HA) composite was synthesized at room temperature using a vortex mixer. Graphite powder, calcium nitrate tetrahydrate and diammonium hydrogen phosphate were used as precursors. The composite was characterized using X-ray diffraction (XRD), Fourier transform infrared spectroscopy (FTIR), Raman spectroscopy, Scanning electron microscopy (SEM), Energy dispersive X-ray Spectroscopy (EDX) and Thermo-Gravimetric analysis (TGA). The nanocrystalline structure of the composite is confirmed by the XRD analysis with an average crystallite size of 13.06 nm and the absence of the –OH absorption band near 3500 cm^{-1} is revealed in the FTIR analysis. The presence of folded and wrinkled RGO sheets are confirmed by SEM images. EDX analysis identified a Ca/P atomic ratio of 1.59, while TGA demonstrated extended thermal stability up to 500˚C, highlighting the composite's potential for biomedical engineering applications.

Keywords— *Graphene oxide (GO), Reduced graphene oxide (RGO), Hydroxyapatite (HA), Biomedical Application*.

Introduction

Hydroxyapatite (HA) with a chemical composition of $[Ca_{10}(PO_4)_6(OH)_2]$ is a calcium phosphate and its chemical composition is similar to the mineral crystallites present in human bone. Due to its unique properties like biocompatibility, bioactivity and osteo-conductivity, it has applications in many important areas like biomaterials science, tissue engineering, biomedicine, energy and environmental science and analytical science [1], [2]. HA implants or HA coatings have poor fracture toughness and weak wear resistance which are their major drawbacks [3]. One possible solution to this problem is the reinforcement of HA by a mechanically robust material that can help in improving the fracture toughness and wear resistance of the HA matrix. A number of different studies have shown the use of graphene and its derivatives to improve the mechanical and biological properties of HA [1], [2], [3]. The results of these works showed that the mechanical and biological properties of HA were improved by the addition of graphene and its derivatives. Graphene and its derivatives worked as a filler that blocked the cracks that grow in the two-dimensional HA structure [4].

© Journal of Gono Bishwabidyalay All Rights Reserved

Graphene in its defect-free form shows some important characteristic such as high conductivity, transparentness, high flexibility, light in weight, and mechanical toughness. However, largescale, defect free graphene remains difficult and costly to produce [5]. The chemical reduction of graphene oxide (GO) produces reduced graphene oxide (RGO) which contains a fraction of sp^3 carbon and residual oxygen-containing functional groups. RGO exhibits more structural defects and significantly lower electrical conductivity than pristine graphene.

Graphene oxide (GO) is an easy-to-make material that has a similar structure. It is a compound consisting of carbon, oxygen, and hydrogen in variable ratios, which can be synthesized by treating graphite with strong oxidizers. Graphene Oxide (GO) is one of the most promising nanocarbon materials. GO is a chemical derivative of graphene, in which basal plane and boundaries are covered by multiple oxygen-containing functional groups [6]. If graphene oxide can be completely reduced, then the product would be graphene. In practice, some oxygen-containing functional groups will remain and not all sp^3 bonds will return to sp^2 configuration [7]. Different reducing agents will lead to different carbon to oxygen ratios and different chemical compositions in reduced graphene oxide. This incomplete reduction of GO is called reduced graphene oxide (RGO). The production of RGO from GO can be carried out by reducing oxygen containing functional groups through thermal, chemical, photochemical, or microbial/bacterial treatments. Recent studies are carried out on RGO-HA and other graphene bioceramic composites with different approach including in-situ hydrothermal methods [8], [9], additive-assisted hydrothermal synthesis [10], and shear-dispersion combined with spark plasma sintering [11] particularly to enhance mechanical properties and expand biomedical applications. These continuous developments signify the ongoing research interest in RGO-HA composites and their potential for advanced biomedical applications.

The aim of this study is to create a composite material that overcomes the existing limitations and disadvantages of HA while improving the mechanical and biological properties and will be useful in the field of biomedical applications.

Experimental

Synthesis of Graphene oxide (GO)

In this present research work, graphene oxide was synthesized by modified Hummer's method. Modified Hummer's method involves both oxidation and exfoliation of graphite sheets due to thermal treatment of solution. In this method of graphene oxide preparation, 5 g of fine graphite powder, 2.5 g of $NaNO_3$, and 115 mL of H_2SO_4 were added in a round bottom flask and stirred for 30 minutes. The mixture was then placed in an ice bath below 20 ºC and 15 g of $KMnO_4$ was added very slowly to the sample with continuous stirring for 3 hours. After that, the ice bath was removed and the mixture was heated at 45°C for 1 hour, and then 230 mL of DI water was added and stirred for another 30 minutes at 45 °C to produce a deep brown reaction mixture. The reaction mixture was then transferred to a beaker and washed with 400 mL of DI water. Here, 30% H_2O_2 was added and stirred for 30 minutes,

and the colour changed to bright yellow. After that 5% HCl was added and stirred for 10 minutes. The solution was left to reach room temperature before being washed with an additional 25 mL of 9:1 DI water to HCl acid to remove metal ions and acids. The mixture was centrifuged at 10000 rpm for 30 minutes at room temperature. The washing was repeated many times using deionized water to wash out the acid. The pH was checked continually and the washing was stopped once the solution reached a neutral pH [12], [13]. The final washed solution was then dried in an oven at 80ºC for 12 hours and then ground using a mortar and pestle to obtain the final powder form of graphene oxide.

Synthesis of Reduced Graphene oxide (RGO)

For reduced graphene oxide (RGO) preparation, a mixture of 0.5 g of GO powder and 500 mL of DI water was prepared. The prepared mixture was sonicated in water for 2 hours and then heated to 80 °C. Next, 0.25 mL of hydrazine hydrate was added to the dispersion. The mixture was kept at 80°C by using a water bath and was subjected to continuous stirring for 72 hours. The mixture was then transferred into centrifuge tubes for cleaning. The cleaning process was done by adding DI water and centrifuging at 10000 rpm for 10 minutes. These steps were repeated several times until the pH became neutral. The final solution was then dried in an oven at 80ºC for 24 hours. The dried sample was then ground using a mortar and pestle to obtain the powder form of RGO.

Despite being toxic in nature, hydrazine hydrate was utilized due to its high efficiency in deoxygenating GO [2]. To reduce the toxicity, the composite was subjected to extensive repeated washing and centrifugation until reaching a neutral pH. This composite can be used in biomedical applications after the confirmation of hydrazine removal by elemental/XPS analysis and in vitro biocompatibility testing because hydrazine is classified as a probable human carcinogen. Our future studies will utilize greener reducing agents (e.g., ascorbic acid or plant-extract-based reductants) as alternatives to hydrazine hydrate for biomedical-grade RGO production.

Synthesis of Hydroxyapatite (HA)

The synthesis of hydroxyapatite was carried out via the wet chemical precipitation method. This synthesis method of hydroxyapatite required two different analytical-grade precursor substances which are calcium nitrate tetra-hydrate (Ca $(NO_3)_2.4H_2O$) and di-ammonium hydrogen phosphate ($(NH_4)_2HPO_4$). Then sodium hydroxide (NaOH) was used to control the pH of the solution [14]. First, the salts required for this method were weighed according to the molar ratio of hydroxyapatite which is 1.67. 0.5 M of Ca $(NO_3)_2.4H_2O$ and 0.5 M of $(NH_4)_2HPO_4$ were used as precursor materials for preparing the hydroxyapatite ($Ca_{10}(PO_4)_6(OH)_2$) nano-particles. Here, 3.0 M NaOH was used as a co-precipitation agent. The solutions of the relevant salts were prepared by mixing them with DI water. Then the solutions of $Ca(NO_3)_2.4H_2O$ and $(NH_4)_2HPO_4$ were mixed under continuous stirring. After stirring for approximately 2 hours, 3.0 M of NaOH was added dropwise to control the pH at 10.00 of the solution. The pH of the solution was observed using a digital pH meter. A thermometer was also used to monitor the temperature of the solution. Next heat was applied with continuous stirring by using a magnetic stirrer and a heater. When the pH of the mixed

solution decreased with increasing temperature, extra NaOH solution was added to keep the value of pH at 10.00. When the temperature reached 40ºC, the procedure was stopped. The final pH of the solution was observed at 10.00 after completing the operation. A large amount of NaOH solution remained in the mixture. To remove the additional NaOH solution, the mixture solution was taken into a centrifuge tube and kept inside the centrifuge rotor. The centrifugation was operated at 10000 rpm for 15 minutes. After repeating the process several times, it is assumed that the NaOH solution was satisfactorily removed. After the centrifugation process, the precipitated hydroxyapatite, $Ca_{10}(PO_4)_6(OH)_2$, was collected in a glass beaker. Then the specimen was heated at 60ºC for 72 hours to remove the water associated with it. Finally, the heated sample was collected and ground with a mortar and pestle to obtain a fine powder.

RGO-HA Composite Preparation

For the preparation of RGO-HA composite, a solution of RGO was prepared by adding 0.2 g of RGO powder into 40 mL of DI water. Then the solution was sonicated by an ultrasonic sonicator for 2 hours at room temperature. Another solution of HA powder was prepared by adding 0.2 g of HA into 40 mL of DI water and the solution was stirred for 30 minutes. The two solutions were mixed and transferred into falcon tubes. The colloidal dispersions of RGO and HA solutions were vigorously mixed using a vortex for 15 minutes and slowly dried at room temperature for seven days, which results in the RGO-HA composite.

This study utilized bulk characterization techniques like (XRD, FTIR, Raman, SEM, EDX, TGA) and no mechanical properties of the composite were evaluated. To ensure that RGO-related structural, spectroscopic, and thermal signatures were highly detectable by these techniques, the composite was prepared with a 1:1 (50 wt%) RGO to HA mass ratio. In the literature, the 0.1–5 wt% range is typically optimized for mechanical reinforcement of HA, which is significantly lower than the prepared composite with a 1:1 (50 wt%). Systematic variation of the RGO content within the literature optimized range, together with mechanical characterization, is a priority for future study.

Result and Discussions

X-ray diffraction analysis

X-ray Diffraction analysis was carried out to study the structure of graphene oxide (GO), reduced graphene oxide (RGO), hydroxyapatite (HA), and reduced graphene oxide - hydroxyapatite (RGO-HA) composite. Figure-1 shows the X-ray diffraction patterns for graphite, graphene oxide, and reduced graphene oxide. The diffraction peak of pure graphite is found at 26.62° with the (002) orientation. This peak indicates the highly organized layer structure of graphite with an interlayer distance of 3.34 Å.

For GO, the peak at 26.62° disappears, and the peak at 11.42°, corresponding to the (001) crystal plane, appears. This indicates that the product is completely oxidized after the chemical oxidation and exfoliation [13].

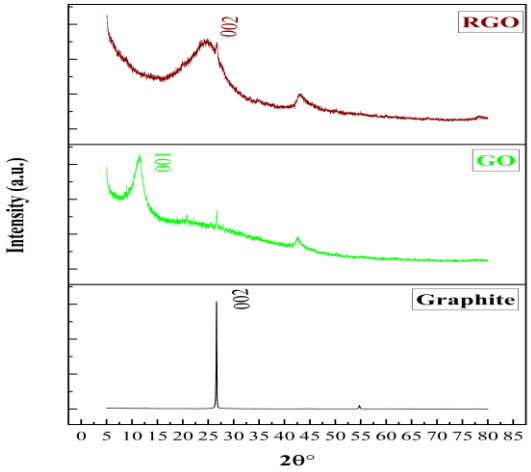


Figure-1: XRD of graphite, GO, RGO, HA and RGO-HA composite.

An increase in d-spacing from 3.34 Å to 7.74 Å shows how the graphene sheets are exfoliated. This increase in interlayer distance is due to the entrapping of oxygen functional groups between the graphene oxide sheets [5]. During the chemical reduction of GO to form RGO, a broader peak has appeared for RGO at 25.26° corresponding to the (002) crystal plane. The diffraction peak of GO at 11.42° corresponding to (001) crystal plane disappeared completely, indicating that the GO was reduced by hydrazine hydrate [15]. The interlayer distance is observed as 3.52 Å, which is lower than that of GO due to the removal of oxygen-containing functional groups and agglomeration of reduced graphene oxide sheets. From the figure it can be seen that the XRD pattern of RGO is not smooth and that small peaks are present which likely occurs because the RGO sheet's structure is affected by the residual functional groups [16].

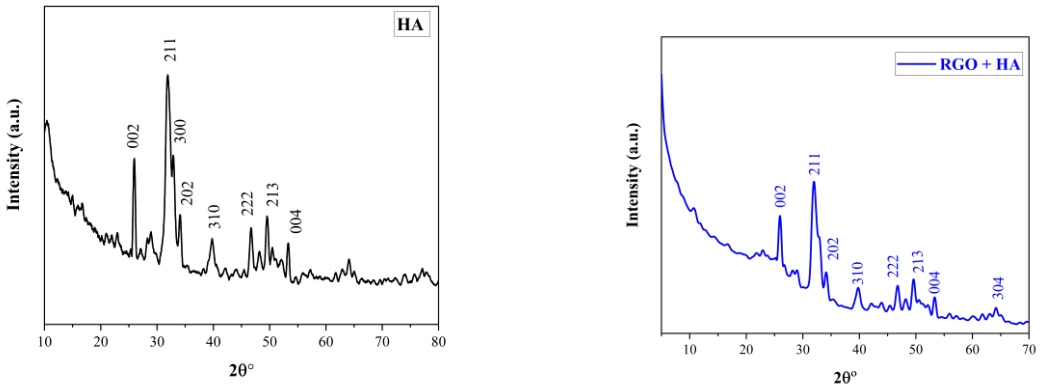


Figure-2: XRD of (a) HA and (b) RGO-HA composite.

Figure-2(a) represents the X-ray diffraction patterns for hydroxyapatite (HA). The crystalline phase of HA is identified by comparing the pattern of diffraction with standard JCPDS card no. 09432 [17]. The characteristics planes for hydroxyapatite are indexed as (211), (112), and (300). However, in this case, the (112) plane cannot be detected in the XRD pattern of prepared hydroxyapatite due to its poor crystallinity. The (211) reflection peaks from the XRD pattern were used to calculate the crystallite size of the hydroxyapatite nanoparticles. The average crystallite size was also calculated and was found as 15.71 nm.

The XRD pattern of RGO-HA composite shows the characteristic peaks of the HA hexagonal phase and found to be consistent with the standard HA diffraction pattern. The diffraction peak of RGO could not be found in the XRD pattern of RGO-HA composite, because the diffraction peaks of HA particles were much stronger than that of RGO. The RGO peak is covered by the HA (002) peak which is highly intensified due to its high crystallinity [18]. The average crystallite size of HA in the composites was calculated by the Scherrer equation as 13.06 nm which is smaller than several recently reported HA-RGO composite crystallite sizes. Rietveld refinement for an in-situ hydrothermal HA-RGO composite reported 28.1 nm [9] and the 16-27 nm range reported for hydrothermally synthesized HA-RGO powders depending on additive use [10]. These values are consistent with the low-temperature and non-sintered precipitation process used in this current study. Due to the heterogeneous nucleation on RGO–HA composite, a slight decrease in HA crystallite size from 15.71 nm (pure HA) to 13.06 nm (RGO–HA composite) is observed [10], [19].

Fourier Transform Infrared Spectroscopy (FTIR) Analysis

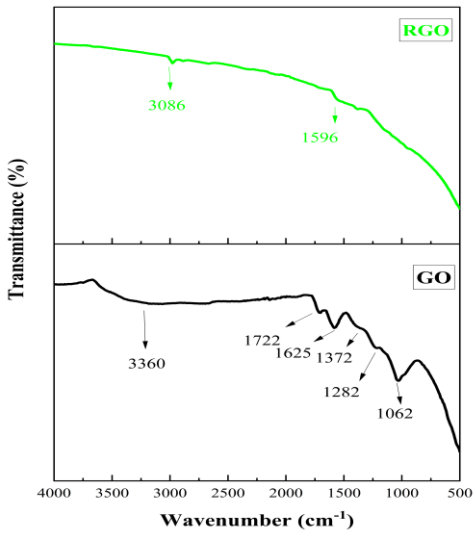


Figure-3: FTIR spectra of prepared GO and RGO.

The GO FTIR spectra show the intense and broad peak at 3360 cm^{-1} which is due to the stretching mode of the -OH bond (hydroxyl group) vibration [15]. The carbonyl groups are

shown at 1722 cm^{-1} as C=O stretching. There is an aromatic C=C group at around 1625 cm^{-1}, which is assigned to the vibrations of absorbed water molecules and also skeletal vibrations of non-oxidized graphitic domains [20]. The peak at 1372 cm^{-1} is due to the stretching of C-OH. The C-O-C bending mode is confirmed by the peak at 1282 cm^{-1}. The presence of oxide functional groups after the oxidation process is confirmed by the stretching of the C-O group which is observed at 1062 cm^{-1} [13].

The reduced graphene oxide (RGO) was confirmed by the reduction in intensity of the peaks that contain oxygen-containing functional groups as shown in Figure-3. The intensity of the epoxy group peak is decreased, which confirms the reduction of oxygen functional groups to form RGO. Here the absorption due to the C=O group (1722 cm^{-1}) is found to be decreased very much in intensity which confirms the removal of the carboxylic group upon reduction. An absorption band that appears at 1596 cm^{-1} may be attributed to the skeletal vibration of the reduced graphite oxide [16]. Table-1 represents the different functional groups with their corresponding wavenumbers.

Table-1: Functional groups and their corresponding bands in prepared Graphene Oxide (GO):

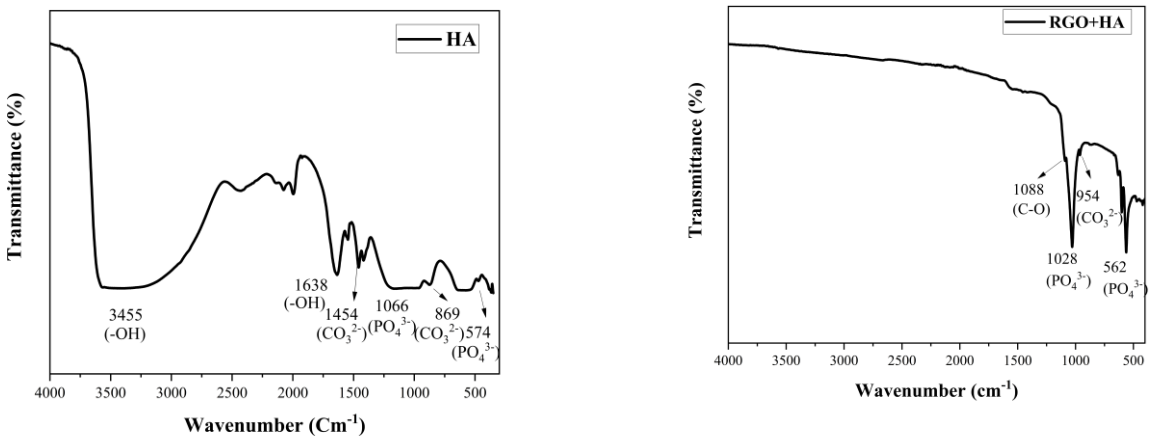
Wavenumber of the corresponding functional group (cm^{-1})	**Stretching or bending mode**	**Functional group**
3360	Stretching mode	-OH (hydroxyl group)
1722	Stretching mode	C=O (carbonyl)
1625	Stretching mode	C=C (Medium)
1372	Stretching mode	C-OH (Carboxyl)
1282	Bending	C-O-C (Epoxy)
1062	Stretching	C-O (Alcoxy)

In the FTIR spectrum of HA, different bands represent different groups. A broad peak around 3455 cm^{-1} refers to the stretching mode of the hydroxyl group (OH-) in the hydroxyapatite crystal. The peak at 1638 cm^{-1} is assigned to the bending of hydroxyl ion due to the chemical absorbance of H_2O. The characteristics of hydroxyapatite nano-powder fabricated by wet chemical precipitation technique have approximately matched the characteristics of the prepared sample [21]. The carbonate functional group $(CO_3)^{2-}$ asymmetric stretching is identified by the 1454 cm^{-1} band and the peaks around 869 cm^{-1} occurs due to the out-of-plane bending of the carbonate group [22]. The missing structural OH stretching band in the FTIR spectrum of HA at around 3572 cm^{-1} is a well-documented characteristic of nanoscale, defective Calcium Deficient Hydroxyapatite (CDHA) [23], [24]. Table-2 represents the analyzed functional groups and their corresponding absorption bands.

Table-2: Functional groups and their corresponding bands of prepared Hydroxyapatite.

Wavenumber of the corresponding functional group (cm^{-1})	**Stretching or bending mode**	**Functional group**
3455	Stretching mode $OH-$ due to absorbed H_2O	$OH-$
1638	Bending of *OH-* due to chemically absorbance of H_2O	*OH-*
1454	Stretching mode of CO_3^{2-} for dissolving CO_2	CO_3^{2-}
1066	Asymmetric stretching	PO_4^{3-}
869	Out of plane bending	CO_3^{2-}
574	Asymmetric bending	PO_4^{3-}

The FTIR spectrum of prepared RGO-HA composite shows the absence of the –OH band at around 3500 cm^{-1} indicates the elimination of the hydroxyl group due to water. The peak



(a) **(b)**

Figure-4: FTIR spectra of prepared (a) HA and (b) RGO-HA composite.

located at 1088 cm^{-1} is due to the C-O stretching vibration. This peak shows a solid indication of the formation of the RGO-HA composite [17]. The peak located at the wavenumber of 1028 cm^{-1} is related to asymmetric stretching of PO_4^{3-} ion. The peaks around 954 cm^{-1} have occurred due to the out of plane bending of carbonate group. Peak located at 562 cm^{-1} indicates antisymmetric deformation due to phosphate ions [25].

Raman Spectroscopy Analysis

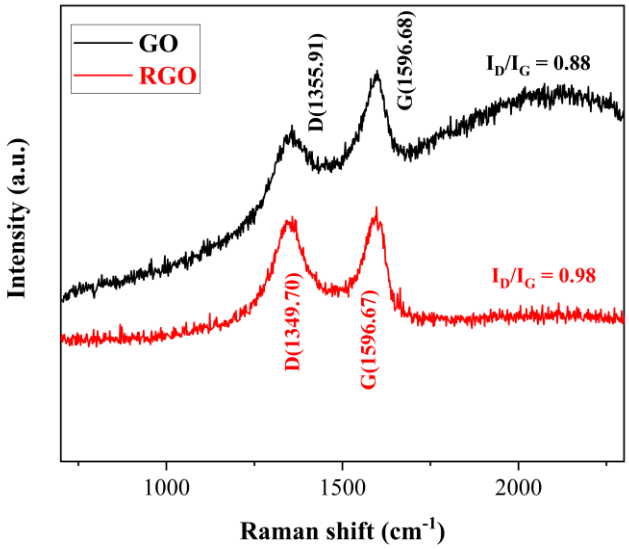
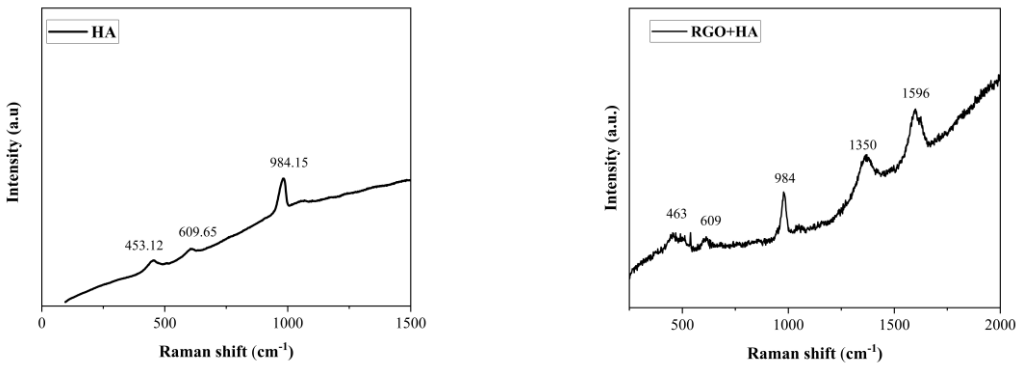


Figure-5: Raman spectroscopy of prepared GO and RGO.

Raman spectroscopy is widely considered as a well-established technique to identify the structural and electronic properties of graphene-based materials. The Raman spectrum provides useful information on defects, carbon sp^2 vibrations, and stacking order. Raman spectroscopy was used to estimate the degree of GO reduction in the RGO sample and to find structural differences between them. Two fundamental vibrations can be observed in the range of 1200 and 1700cm^{-1} for GO and RGO. The D vibration band is formed from a



(a) **(b)**

Figure-6: Raman spectroscopy of prepared (a) HA and (b) RGO-HA composite.

breathing mode of κ-point photons of A_{1g} symmetry [26]. On the other hand, G vibration band arises from the first-order scattering of E_{2g} phonons by sp^2 carbon. Furthermore, the G vibration band is also contributed by the presence of the stretching C-C bond, which is

common in all sp^2 carbon systems [27]. The D band and G band in the Raman spectrum symbolize the disorder bands and the tangential bands, respectively. Therefore, the intensity of the D peak is used to measure the degree of disorder.

The D vibration band can be seen at 1355.91 and 1349.70 cm^{-1} for GO and RGO, respectively. On the other hand, the G vibration band from the first-order scattering of E_{2g} phonons by sp^2 carbon appeared at 1596.68 cm^{-1} for GO and 1596.67 cm^{-1} for RGO. The lower relative intensity of the D (1349.70 cm^{-1}) to G (1596.67 cm^{-1}) band implies that the obtained RGO is mainly composed of well-crystallized graphite [25]. The ratio of the intensities of the D and G bands (I_D/I_G) determines the reduction degree of GO and provides information about the changes in the sp^2 and sp^3 hybridization domains in the carbon lattice. The increase in I_D/I_G value from 0.88 (GO) to 0.98 (RGO) indicates a large number of defects in the crystal lattice, and also the chemical reduction [20].

The Raman spectroscopy of prepared HA shows a peak at 453.12 cm^{-1} which is due to the v_2 symmetrical bending vibration of phosphate (PO_4^{3-}) ions while the peak at 609.65 cm^{-1} represents the v_3 asymmetrical stretching mode of phosphate (PO_4^{3-}) ions. The characteristic peak of the nano-sized crystalline HA phase at 984.15 cm^{-1}, is assigned to the symmetric stretching $v_1(PO_4^{3-})$ of free tetrahedral phosphate ions [18], [22]. So, prepared HA was dominated by several noticeable bands near 453.12, 609.65, and 984.15 cm^{-1}, which was due to the characteristic peaks of the phosphate groups abundant in HA.

For prepared RGO-HA composite, the peaks at 463, 609, 984 cm^{-1} are observed. These peaks represent the characteristic peaks of the phosphate groups abundant in HA [28]. In addition, characteristic peaks of RGO were found near 1350 cm^{-1} for the D band and at 1596 cm^{-1} for the G band. These characteristic peaks of HA and RGO did not shift in RGO-HA composites after coating. Therefore, it was confirmed that RGO was firmly coated on the surface of HA. The D and G peaks in the RGO have not had any significant displacement at the Raman spectra of RGO-HA composites which also indicate that the RGO-HA powders have been successfully synthesized [18].

Scanning Electron Microscopy (SEM) Analysis

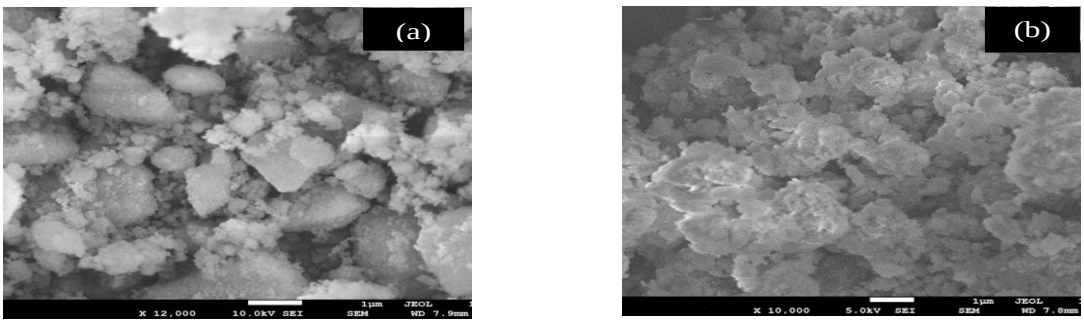


Figure-7: SEM image of prepared (a) HA and (b) RGO-HA composite.

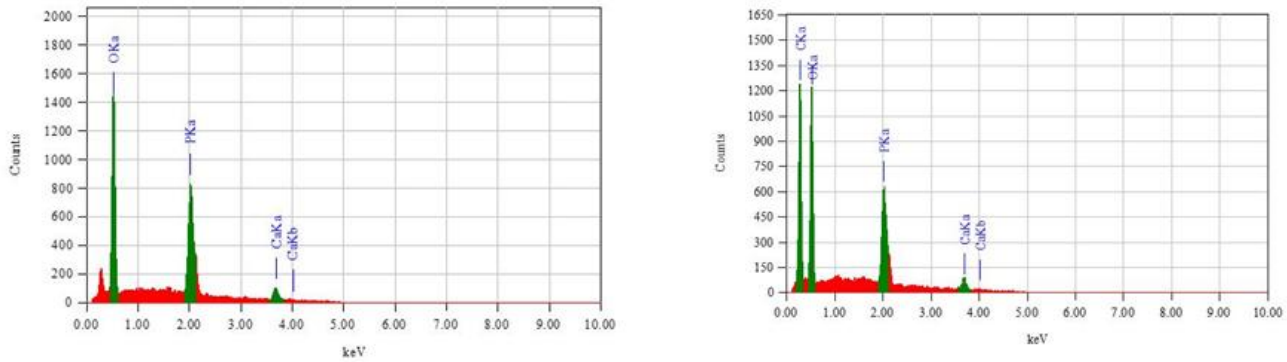
Figure-7 (a) shows the morphology and particle size of the synthesized HA powder. SEM pattern gives insight into the HA structure with respect to particle size and shape. There are a few very large particles on the micrometer scale due to agglomeration. Agglomeration occurs due to the high surface energy of HA [21]. The particle sizes of HA are found to be in the range of 0.09–1.5 µm. Due to the particle agglomeration during precipitation and subsequent drying, relatively broad particle-size is observed [29].

From the SEM image of the synthesized hydroxyapatite, the porous nature of HA is also observed. This porous nature is a desirable property and can have a positive impact when used in the implant as it facilitates interaction between the implant and the biological environment [30].

Figure-7 (b) shows the SEM image of prepared composite. It shows the growth of HA on two-dimensional RGO sheets. The HA particles have agglomerated in some places. SEM images also show the agglomeration-free HA nano-particles spread on the reduced graphene oxide sheets and HA particles were partly wrapped and interconnected by the RGO network through weakly bonded Van der Waals interactions [22]. The surface potential of RGO is negatively charged due to the hydroxyl and carboxyl groups on their surface, whereas HA is positively charged because of its calcium moieties [31].

Energy dispersive X-ray Spectroscopy (EDX) analysis

EDX data shows that the Ca/P ratio is approximately 1.56 for the prepared HA which is consistent with biogenic bone mineral typically exhibiting a Ca/P ratio between 1.50 and 1.67 [14], [32]. HA with a high Ca/P ratio degrades much faster, which is not suitable for biological applications.



(a) **(b)**

Figure-8: EDX of prepared (a) HA and (b) RGO-HA composite.

Table-3: Elements of Hydroxyapatite (EDX Data)

Element	**Atom (%)**
Oxygen (O)	44.70
Phosphorus (P)	21.64
Calcium (Ca)	33.66
Total	100

For the composite, the presence of carbon, oxygen, phosphorus, and calcium is confirmed by EDX data. The composite EDX data shows 31.22% carbon mass fraction which is attributed to environmental adventitious carbon and sample preparation artifacts. The ratio Ca/P is observed as 1.59 which signifies the formation of Calcium Deficient Hydroxyapatite (CDHA). The CDHA mimics natural bone closer than highly crystalline stoichiometric HA with superior bioactivity, increased solubility, and enhanced osteoconductivity which is highly advantageous for promoting bone integration and implant resorption [33].

Table-4: Elements of RGO-HA Composite (EDX Data).

Element	**Atom (%)**
Carbon (C)	31.22
Oxygen (O)	31.62
Phosphorus (P)	14.33
Calcium (Ca)	22.83
Total	100

Thermogravimetric Analysis (TGA)

Thermogravimetric analysis (TGA) is an analytical technique that is used to determine a material's thermal stability and its fraction of volatile components by monitoring the weight change that occurs as a sample is heated at a constant rate.

Figure-9 shows the TGA curves of GO, RGO, HA, and RGO-HA composite from room temperature to 800 $^{\circ}$C at a heating rate of 10 $^{\circ}$C min^{-1} under a nitrogen atmosphere. Due to the thermal instability of GO, it starts to lose mass upon heating even below 100 ºC [34]. The initial weight loss below 100 °C for GO is due to the removal of water molecules adsorbed on the surface of GO [3]. The major weight loss that occurs at around 200 $^{\circ}$C is due to the pyrolysis of the labile oxygen-containing functional groups, yielding CO, CO_2, and steam [34]. A flat weight loss was observed between 200 and 800 °C, which can be referred to as

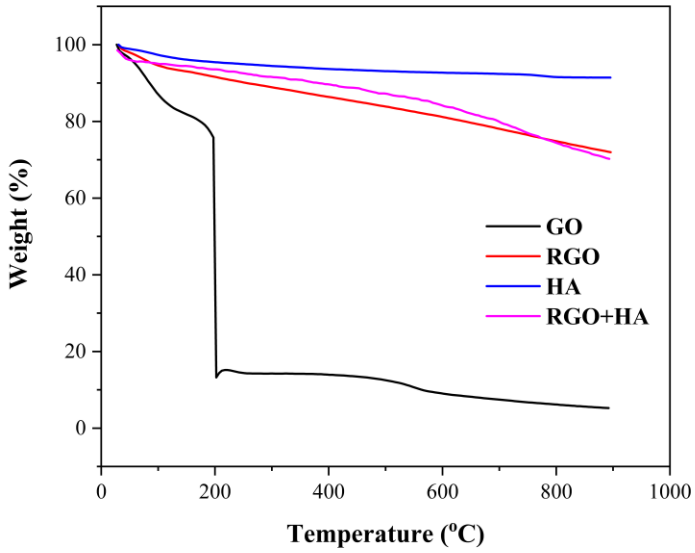


Figure-9: TGA graph of graphene oxide (GO), reduced graphene oxide (RGO), Hydroxyapatite (HA), and reduced graphene oxide – hydroxyapatite (RGO-HA) composite.

the removal of more stable oxygen functionalities. In the case of RGO, the removal of the thermally labile oxygen functional groups by chemical reduction results in much increased thermal stability for the RGO. A slight weight loss is observed below 100 °C, which can be attributed to the loss of adsorbed water [34]. When this material is heated up to 800 °C, no significant weight loss is observed. The synthesized HA suffered a very slow weight loss process from room temperature to 800 °C. The initial weight loss at around 100 °C is attributed to the evaporation of absorbed water [35]. For pure HA the weight loss in the range of 30–100 °C is mainly due to the physically and weak chemically bound water [1]. The composite contains a very small amount of water because of the complete reduction of GO. The curve of the composite showed that the sample had lost a very small amount of mass up to 500°C. After 500°C, the heavy mass loss occurs compared to pure HA between 500 and 800°C. This behavior is attributed to progressive thermal decomposition of the residual RGO carbon framework and any remaining oxygen-containing functional groups, consistent with the high carbon content (31.22%) confirmed by EDX analysis [17]. The HA phase does not show any significant thermal degradation and remains thermally stable till 800 °C even after the addition of RGO. Hence, the overall TGA profile of the composite is a result of individual TGA behavior of its components.

Conclusion and Future Directions

In the present work, reduced graphene oxide-hydroxyapatite (RGO-HA) composite was synthesized at room temperature by the physical combination of RGO prepared by the modified Hummer's method followed by hydrazine reduction with HA prepared by wet chemical precipitation. The existence of a nanocrystalline, carbonate-substituted, calcium-deficient HA phase with RGO in the composite is confirmed by XRD, FTIR, Raman, SEM,

EDX and TGA results. Furthermore, SEM analysis showed that the RGO sheets cover and decorate the HA particles partially. The crystallite size of HA (13.06 nm) and the Ca/P ratio (1.59) for the composite are in close agreement with the values reported for other low-temperature, non-sintered RGO-HA systems in the current literature, confirming the present synthesis method, but indicating the need for further optimization for biomedical-grade efficacy. However, these structural and thermal properties are not sufficient on their own to determine the suitability of the composite for biomedical applications. Further studies on key mechanical properties such as hardness and fracture toughness and biological properties such as cytotoxicity, bioactivity and osteogenesis induction potential, should be carried out. Also, the RGO concentration used in the present composite (50 wt%) is much higher than the range of 0.1-5 wt% reported in the literature for effective reinforcement. Future efforts will be directed toward optimizing the concentration of RGO, complete removal of hydrazine and systematic in vitro biocompatibility and mechanical evaluations to conclusively establish the therapeutic potential of the material.

Authors Contributions

Conceptualization, study design and writing-original draft were contributed by Md. Tushar Ahmed. Data entry, table and figure preparation were done by Md. Mostafa Kamal. All authors have read and agreed to the published version of the manuscript.

Acknowledgements

The authors would like to express their sincere gratitude to the Atomic Energy Centre, Dhaka (AECD), Dhaka-1000 and Department of Physics, Gono Bishwabidyalay Savar, Dhaka-1344 for their constant support to complete this article.

Conflict of interest

The authors declare that they do not have any conflict of interest.

References

1. R. Barabás et al., “Graphene Oxides/Carbon Nanotubes–Hydroxyapatite Nanocomposites for Biomedical Applications,” Arabian Journal for Science and Engineering, vol. 45, no. 1, pp. 219–227, Jul. 2019, doi: 10.1007/S13369-019-04058-4.
2. G. Wei, C. Gong, K. Hu, Y. Wang, and Y. Zhang, “Biomimetic Hydroxyapatite on Graphene Supports for Biomedical Applications: A Review,” Nanomaterials, vol. 9, no. 10, p. 1435, Oct. 2019, doi: 10.3390/NANO9101435.
3. G. M. Neelgund, A. Oki, and Z. Luo, “In situ deposition of hydroxyapatite on graphene nanosheets,” Mater. Res. Bull., vol. 48, no. 2, pp. 175–179, Feb. 2013, doi: 10.1016/J.MATERRESBULL.2012.08.077.
4. K. Olszowska et al., “Three-dimensional nanostructured graphene: Synthesis and energy, environmental and biomedical applications,” Synth. Met., vol. 234, pp. 53–85, Dec. 2017, doi: 10.1016/J.SYNTHMET.2017.10.014.
5. H. Saleem, M. Haneef, and H. Y. Abbasi, “Synthesis route of reduced graphene oxide via

thermal reduction of chemically exfoliated graphene oxide," Mater. Chem. Phys., vol. 204, pp. 1–7, Jan. 2018, doi: 10.1016/J.MATCHEMPHYS.2017.10.020.
6. T. Tiliakos, A. Cucu, C. Ceaus, A. M. I. Trefilov, E. C. Serban, and I. Stamatin, "Graphite Oxide Post-Synthesis Processing Protocols," Int. J. Sci. Commun., 2015, doi: 10.13140/RG.2.1.2452.9041.
7. "Nanotechnologies—Vocabulary—Part 13: Graphene and related two-dimensional (2D) materials," 2017. [Online]. Available: https://standards.iteh.ai/catalog/standards/sist/da226f74-58d3-4f1c-8e60-
8. B. Flora et al., "Development of chemically synthesized hydroxyapatite composite with reduced graphene oxide for enhanced mechanical properties," J. Mech. Behav. Biomed. Mater., vol. 142, p. 105845, Jun. 2023, doi: 10.1016/J.JMBBM.2023.105845.
9. J. J. Ruíz-Osorio et al., "In Situ Synthesis of a Hydroxyapatite and Reduced Graphene Oxide Composite for Potential Electrochemical Biosensing Applications," ACS Omega, vol. 10, no. 27, pp. 29680–29689, Jul. 2025, doi: 10.1021/ACSOMEGA.5C03514.
10. H. Nosrati, R. Sarraf-Mamoory, M. Canillas Perez, D. Q. S. Le, R. Zolfaghari Emameh, and C. E. Bünger, "Characteristics of hydroxyapatite-reduced graphene oxide composite powders synthesized via hydrothermal method in the absence and presence of diethylene glycol," Open Ceramics, vol. 5, p. 100067, Mar. 2021, doi: 10.1016/J.OCERAM.2021.100067.
11. B. Y. Wang, S. Hsu, C. M. Chou, T. I. Wu, and V. K. S. Hsiao, "Improved Mechanical Properties of Ultra-High Shear Force Mixed Reduced Graphene Oxide/Hydroxyapatite Nanocomposite Produced Using Spark Plasma Sintering," Nanomaterials, vol. 11, no. 4, p. 986, Apr. 2021, doi: 10.3390/NANO11040986.
12. R. Al-Gaashani, A. Najjar, Y. Zakaria, S. Mansour, and M. A. Atieh, "XPS and structural studies of high quality graphene oxide and reduced graphene oxide prepared by different chemical oxidation methods," Ceram. Int., vol. 45, no. 11, pp. 14439–14448, Aug. 2019, doi: 10.1016/J.CERAMINT.2019.04.165.
13. P. B. Arthi G and L. BD, "A Simple Approach to Stepwise Synthesis of Graphene Oxide Nanomaterial," J. Nanomed. Nanotechnol., vol. 6, no. 1, 2015, doi: 10.4172/2157-7439.1000253.
14. S. Mondal, A. Dey, and U. Pal, "Low temperature wet-chemical synthesis of spherical hydroxyapatite nanoparticles and their in situ cytotoxicity study," Adv. Nano Res., vol. 4, no. 4, pp. 295–307, Dec. 2016, doi: 10.12989/ANR.2016.4.4.295.
15. N. M. S. Hidayah et al., "Comparison on graphite, graphene oxide and reduced graphene oxide: Synthesis and characterization," AIP Conf. Proc., vol. 1892, no. 1, Oct. 2017, doi: 10.1063/1.5005764/965987.
16. A. T. Habte, D. W. Ayele, and M. Hu, "Synthesis and Characterization of Reduced Graphene Oxide (rGO) Started from Graphene Oxide (GO) Using the Tour Method with Different Parameters," Advances in Materials Science and Engineering, vol. 2019, p. 5058163, Jan. 2019, doi: 10.1155/2019/5058163.
17. C. Rodríguez-González, H. E. Cid-Luna, P. Salas, and V. M. Castaño, "Hydroxyapatite-Functionalized Graphene: A New Hybrid Nanomaterial," J. Nanomater., vol. 2014, p. 940903, Jan. 2014, doi: 10.1155/2014/940903.
18. H. Nosrati, R. Sarraf-Mamoory, D. Q. S. Le, R. Zolfaghari Emameh, M. Canillas Perez, and

C. E. Bünger, “Improving the mechanical behavior of reduced graphene oxide/hydroxyapatite nanocomposites using gas injection into powders synthesis autoclave,” Scientific Reports, vol. 10, p. 8552, May 2020, doi: 10.1038/s41598-020-64928-y.

19. Y. Liu, J. Huang, and H. Li, “Synthesis of hydroxyapatite-reduced graphite oxide nanocomposites for biomedical applications: oriented nucleation and epitaxial growth of hydroxyapatite,” doi: 10.1039/C3TB00531C.
20. J. Jagiełło, A. Chlanda, M. Baran, M. Gwiazda, and L. Lipińska, “Synthesis and Characterization of Graphene Oxide and Reduced Graphene Oxide Composites with Inorganic Nanoparticles for Biomedical Applications,” Nanomaterials, vol. 10, no. 9, p. 1846, Sep. 2020, doi: 10.3390/NANO10091846.
21. V. Rodríguez-Lugo et al., “Wet chemical synthesis of nanocrystalline hydroxyapatite flakes: effect of pH and sintering temperature on structural and morphological properties,” R. Soc. Open Sci., vol. 5, no. 8, p. 180962, Aug. 2018, doi: 10.1098/RSOS.180962.
22. G. Bharath et al., “Enzymatic electrochemical glucose biosensors by mesoporous 1D hydroxyapatite-on-2D reduced graphene oxide,” J. Mater. Chem. B, vol. 3, no. 7, pp. 1360–1370, Feb. 2015, doi: 10.1039/C4TB01651C.
23. M. Manoj, R. Subbiah, D. Mangalaraj, N. Ponpandian, C. Viswanathan, and K. Park, “Influence of Growth Parameters on the Formation of Hydroxyapatite (HAp) Nanostructures and Their Cell Viability Studies,” Nanobiomedicine (Rij)., vol. 2, p. 2, Feb. 2015, doi: 10.5772/60116.
24. N. A. M. Barakat et al., “Physiochemical characterizations of hydroxyapatite extracted from bovine bones by three different methods: extraction of biologically desirable Hap,” Materials Science and Engineering C, vol. 28, no. 8, pp. 1381–1387, Jan. 2008, doi: 10.1016/J.MSEC.2008.03.003.
25. P. Lian, X. Zhu, S. Liang, Z. Li, W. Yang, and H. Wang, “Large reversible capacity of high quality graphene sheets as an anode material for lithium-ion batteries,” Electrochim. Acta, vol. 55, no. 12, pp. 3909–3914, Apr. 2010, doi: 10.1016/J.ELECTACTA.2010.02.025.
26. S. Thakur and N. Karak, “Green reduction of graphene oxide by aqueous phytoextracts,” Carbon N. Y., vol. 50, no. 14, pp. 5331–5339, Nov. 2012, doi: 10.1016/J.CARBON.2012.07.023.
27. M. S. Dresselhaus, A. Jorio, M. Hofmann, G. Dresselhaus, and R. Saito, “Perspectives on Carbon Nanotubes and Graphene Raman Spectroscopy,” Nano Lett., vol. 10, no. 3, pp. 751–758, Mar. 2010, doi: 10.1021/NL904286R.
28. J. H. Lee et al., “Reduced graphene oxide-coated hydroxyapatite composites stimulate spontaneous osteogenic differentiation of human mesenchymal stem cells,” Nanoscale, vol. 7, no. 27, pp. 11642–11651, Jul. 2015, doi: 10.1039/C5NR01580D.
29. M. Tourbin et al., “Agglomeration of stoichiometric hydroxyapatite: Impact on particle size distribution and purity in the precipitation and maturation steps,” Powder Technol., vol. 360, pp. 977–988, Jan. 2020, doi: 10.1016/J.POWTEC.2019.10.050.
30. S. V. Ganachari, “Rapid synthesis, characterization, and studies of hydroxyapatite nanoparticles.” [Online]. Available: http://www.alliedacademies.org/advanced-materials-science-research/
31. J. H. Lee et al., “Enhanced Osteogenesis by Reduced Graphene Oxide/Hydroxyapatite

Nanocomposites," Scientific Reports, vol. 5, p. 18833, Dec. 2015, doi: 10.1038/srep18833.
32. M. Tavoni, M. Dapporto, A. Tampieri, and S. Sprio, "Bioactive Calcium Phosphate-Based Composites for Bone Regeneration," Journal of Composites Science, vol. 5, no. 9, p. 227, Aug. 2021, doi: 10.3390/JCS5090227.
33. X. Li, Y. Deng, M. Wang, X. Chen, Y. Xiao, and X. Zhang, "Stabilization of Ca-deficient hydroxyapatite in biphasic calcium phosphate ceramics by adding alginate to enhance their biological performances," J. Mater. Chem. B, vol. 6, no. 1, pp. 84–97, Dec. 2017, doi: 10.1039/C7TB02620J.
34. S. Stankovich et al., "Synthesis of graphene-based nanosheets via chemical reduction of exfoliated graphite oxide," 2007, doi: 10.1016/j.carbon.2007.02.034.
35. M. Li et al., "In situ synthesis and biocompatibility of nano hydroxyapatite on pristine and chitosan functionalized graphene oxide," J. Mater. Chem. B, vol. 1, no. 4, pp. 475–484, Jan. 2013, doi: 10.1039/C2TB00053A.